

# UC Irvine

## UC Irvine Previously Published Works

### Title

In vivo optical coherence tomography-based scoring of oral mucositis in human subjects: A pilot study

### Permalink

<https://escholarship.org/uc/item/9g54b9j9>

### Journal

J. Biomed. Opt, 12

### Authors

Wilder-Smith, PE  
Kawakami-Wong, H  
Gu, S  
[et al.](#)

### Publication Date

2007-09-30

### Copyright Information

This work is made available under the terms of a Creative Commons Attribution License, available at <https://creativecommons.org/licenses/by/4.0/>

Peer reviewed

# *In vivo* optical coherence tomography–based scoring of oral mucositis in human subjects: a pilot study

**Hilari Kawakami-Wong**  
**Shuguang Gu**  
**Marie J. Hammer-Wilson**  
University of California, Irvine  
Beckman Laser Institute  
1002 Health Sciences Road East  
Irvine, California 92612

**Joel B. Epstein**  
University of Illinois at Chicago  
College of Medicine  
College of Dentistry and Cancer Center  
Chicago, Illinois 60612

**Zhongping Chen**  
**Petra Wilder-Smith**  
University of California, Irvine  
Beckman Laser Institute  
1002 Health Sciences Road East  
Irvine, California 92612

**Abstract.** A preliminary study to assess noninvasive optical coherence tomography (OCT) for early detection and evaluation of chemotherapy-induced oral mucositis in five patients. In five patients receiving neoadjuvant chemotherapy for primary breast cancer, oral mucositis was assessed clinically, and imaged using noninvasive OCT. Imaging was scored using a novel imaging-based scoring system. Conventional clinical assessment using the Oral Mucositis Assessment Scale was used as the gold standard. Patients were evaluated on days 0, 2, 4, 7, and 11 after commencement of chemotherapy. OCT images were visually examined by one blinded investigator. The following events were identified using OCT: (1) change in epithelial thickness and subepithelial tissue integrity (beginning on day 2), (2) loss of surface keratinized layer continuity (beginning on day 4), (3) loss of epithelial integrity (beginning on day 4). Imaging data gave higher scores compared to clinical scores earlier in treatment, suggesting that the imaging-based diagnostic scoring was more sensitive to early mucositic change than the clinical scoring system. Once mucositis was established, imaging and clinical scores converged. Chemotherapy-induced oral changes were identified prior to their clinical manifestation using OCT, and the proposed scoring system for oral mucositis was validated for the semiquantification of mucositic change. © 2007 Society of Photo-Optical Instrumentation Engineers. [DOI: 10.1117/1.2779025]

Keywords: mucositis; imaging; optical coherence tomography; human.

Paper 07055SSR received Feb. 16, 2007; revised manuscript received May 4, 2007; accepted for publication May 17, 2007; published online Sep. 21, 2007.

## 1 Introduction

### 1.1 Oropharyngeal Mucositis

Oropharyngeal mucositis (OM) occurs in 30 to 75% of chemotherapy patients, in up to 75% of patients receiving hematopoietic cell transplant (HCT), and in essentially all patients receiving head and neck radiation in doses over 5000 cGy. Ulcerative mucositis is the most common cause of severe pain in HCT and treatments for hematologic cancer. Although advances in HCT have led to a modest reduction in the frequency of severe oral ulcerative mucositis, changes in treatment of head and neck cancer including combined chemotherapy and irradiation and changes in radiation therapy dosing schedules have increased the severity and duration of mucositis in these patients.<sup>1</sup>

OM may lead to alterations in cancer therapy, dose reduction, delay in scheduled therapy, and may require interruption or termination of planned therapy, with the potential for impact on patient cure. In addition, OM is associated with a negative impact on quality of life (QOL) and increased cost of care.<sup>2–5</sup> OM is the most common distressing and disabling acute complication of cancer chemotherapy,<sup>6</sup> and radiotherapy,<sup>7</sup> as reported by patients, and is among the most

significant major dose-limiting toxicities of cancer therapy.<sup>8,9</sup> Clinically, OM<sup>9</sup> is characterized by mucosal changes, including erythema and ulceration, which cause oropharyngeal pain. Currently, prediction of onset and severity of mucositis is not possible, thereby hampering efforts at targeted intervention and optimizing treatment effectiveness. The inability to characterize and measure mucositis accurately has prevented accurate evaluation of lesions and treatments. The ability to detect early, monitor, and characterize OM would greatly enhance our developing understanding of the pathogenesis of mucositis, leading to improved preventive and treatment strategies and mucosal repair.

### 1.2 Optical Coherence Tomography

Optical coherence tomography (OCT) is a high-resolution optical technique that permits minimally invasive imaging of near-surface abnormalities in complex tissues.<sup>10,11</sup> Conceptually, it has been compared to ultrasound scanning.<sup>12</sup> Both ultrasound and OCT provide real-time structural imaging, but unlike ultrasound, OCT is based on low-coherence interferometry, using broadband light to provide cross-sectional, high-resolution subsurface tissue images.<sup>13–18</sup> Broadband laser light waves are emitted from a source and directed toward a beamsplitter; one wave is sent toward a reference mirror with

Address all correspondence to: Dr. Petra Wilder-Smith, University of California, Irvine, Beckman Laser Institute, 1002 Health Sciences Rd East, Irvine, CA 92612; Tel: 949 824 4713; Fax: 949 824 8413; E-mail: pwsmith@uci.edu

known path length and the other toward the tissue sample. After the two beams reflect off the reference mirror and tissue sample surfaces at varying depths within the sample, the reflected light is directed back toward the beamsplitter, where the waves are recombined and read with a photodetector. The image is produced by analyzing interference of the recombined light waves. Cross-sectional images of tissues are constructed in real time, at near histological resolution (approximately 10  $\mu\text{m}$  with current technology). This permits *in vivo* noninvasive imaging of the microscopic characteristics of epithelial and subepithelial structures, including (1) depth and thickness, (2) histopathological appearance, and (3) peripheral margins. With a tissue penetration depth of 1 to 2 mm, the imaging range of the OCT technology described in this paper is suitable for imaging of the oral mucosa.<sup>19–21</sup> Previous studies using OCT have demonstrated the ability to evaluate characteristics of epithelial, subepithelial, and basement membrane structures and show the potential for near histopathological-level resolution and close correlation with histological appearance.<sup>16–29</sup> Two recent studies have reported the successful use of OCT for the early detection and quantification of radiation- and chemotherapy-induced mucositis in the mouse and hamster models.<sup>30,31</sup>

In this feasibility study, the ability of OCT to detect and characterize chemotherapy-induced oral mucositis was evaluated in five human subjects.

## 2 Materials and Methods

### 2.1 Human Subjects, Clinical and Imaging Procedure

Five female human subjects receiving neoadjuvant chemotherapy for primary breast cancer who had developed oral mucositis during the previous chemotherapy cycle were consented and enrolled in this study as approved under University of California—Irvine's Independent Review Board's approval 2002-2805. The likelihood of developing mucositis is high in patients who have suffered from mucositis during the previous cycle of chemotherapy. Informed written consent was obtained from all patients. After enrollment in this study, and prior to the commencement of the next cycle of chemotherapy, a full oral examination was completed, and baseline photographs of the healthy oral mucosa were taken in the following areas: left and right cheeks, dorsal and ventral surfaces of the tongue, lateral borders of the tongue, upper and lower labial sulci, buccal and labial gingivae. Photographs were immediately printed out, and the scan line locations for the baseline OCT imaging conducted at that time were marked on the photographs. Imaging was performed using a hand-held fiber-optic probe and 6-mm scan lines. Each location was scanned three times to assess the reproducibility of the images obtained. This procedure was repeated at 2, 4, 7, and 11 days after the commencement of chemotherapy. These imaging time points were dictated by patient availability. Ideally the patients would have been imaged daily, especially in the early days immediately after commencement of chemotherapy. Clinical evaluation was documented at each time point using the standard Oral Mucositis Assessment Scale (OMAS) (by one observer, PWS) to assess erythema and ulceration in oral tissue, combined with a visual analog pain scale (VAS) (Tables 1 and 2). OMAS was developed by a working group and validated as published in *Cancer*.<sup>2,3</sup>

**Table 1** Cumulative scoring system in a scale of 0 to 5 for clinical evaluation of mucositis based on OMAS scale.

Ulcer	Redness		
	0	1	2
0	0	1	2
1	1	2	3
2	2	3	4
3	3	4	5

OMAS has been shown to be highly reproducible between observers ( $r > 0.8$ ), responsive over time ( $r > 0.9$ ), and accurately record the anatomic elements considered to be associated with mucositis.<sup>2,3</sup> This scoring tool has since been employed in several multicenter mucositis studies.<sup>2,3,6–9</sup>

### 2.2 OCT

The OCT system included a broadband light source from a 1310-nm superluminescent diode with a full width at half maximum bandwidth of 75 nm. The light was split into reference and sample arms by a 2×2 coupler. In the reference arm, a rapid scanning optical delay line provided group delay without phase modulation. A stable carrier frequency was generated by an electro-optic phase modulator for heterodyne detection. A handheld fiber-optic probe with a collimator, an objective lens driven by a translation stage, and a visible aiming beam (633 nm) were used for image acquisition.

The phase-resolved OCT system used in these studies had the following performance parameters: (1) axial resolution: 10  $\mu\text{m}$ ; (2) axial-scan frequency: 1 to 4 kHz; (3) frame rate: 1 to 8 frame/seconds; (4) imaging depth: 1 to 2 mm. Acqui-

**Table 2** OMAS scale for oral mucositis.

Location	Ulceration <sup>a</sup>	Erythema <sup>b</sup>
<b>Lip—upper</b>	<b>0, 1, 2, or 3</b>	<b>0, 1, or 2</b>
<b>Lip—lower</b>	<b>0, 1, 2, or 3</b>	<b>0, 1, or 2</b>
<b>Buccal mucosa—right</b>	<b>0, 1, 2, or 3</b>	<b>0, 1, or 2</b>
<b>Buccal mucosa—left</b>	<b>0, 1, 2, or 3</b>	<b>0, 1, or 2</b>
<b>Tongue ventrolateral—right</b>	<b>0, 1, 2, or 3</b>	<b>0, 1, or 2</b>
<b>Tongue ventrolateral—left</b>	<b>0, 1, 2, or 3</b>	<b>0, 1, or 2</b>
<b>Floor of mouth</b>	<b>0, 1, 2, or 3</b>	<b>0, 1, or 2</b>
<b>Palate—soft</b>	<b>0, 1, 2, or 3</b>	<b>0, 1, or 2</b>
<b>Palate—hard</b>	<b>0, 1, 2, or 3</b>	<b>0, 1, or 2</b>

<sup>a</sup>Area of ulceration: 0=none, 1 $\leq$ 1 cm<sup>2</sup>, 2=1 to 3 cm<sup>2</sup>, 3 $\geq$ 3 cm<sup>2</sup>.

<sup>b</sup>Severity of erythema: 0=none, 1=not severe, 2=severe.

**Table 3** OCT-based scale for assessing oral mucositis.

## Scoring of OCT-visible mucositis changes

**A. Epithelial thickness**Score 0: Same as day 0 ( $\pm 20\%$ )Score 1: Reduced versus day 0 by  $<50\%$ 

Score 2: Reduced versus day 0 by 50 to 99%

Score 3: Reduced versus day 0 by  $>99\%$  to 100%**B. Loss of surface integrity**

Score 1 if yes.

**C. Loss of subsurface integrity**

Score 1 if yes.

Thus, total scoring range for OCT (structural) lies between 0 and 5.

sition time for each image was  $<1$  s. All OCT images were acquired with  $1200 \times 510$  pixels, which equates with 6 mm (length)  $\times$  1.6 mm (depth) for most tissues.

**2.3 Evaluation of OCT Data**

OCT images were coded to blind the evaluator (PWS) to their source. All images were scored in one session and evaluated for changes in epithelial thickness, loss of surface integrity, and loss of subsurface integrity. These three scores combined to generate one cumulative final score as shown in Table 3. Where several diagnostic scores for any attribute in one lesion were possible due to lesion heterogeneity, the highest (most severe) attribute score that applied to that lesion was used. Due to the small number of subjects, and the exploratory nature of this study, a detailed statistical analysis of the data was not undertaken.

**3 Results****3.1 Clinical Data**

We had anticipated potential movement artifacts during OCT registration in human subjects, however, when patients were seated in a chair with a headrest and neck support, this was not a problem at all, as evidenced by Fig. 1. Changes evident in the oral mucosa following chemotherapy included the following: no clinical changes, mucosal erythema, microulceration, frank open ulceration, surface necrosis and sloughing, mucosal breakdown and healing. On day 2, no clinical evidence of mucositis was observed in any patient. By day 4, mucositis was evident in 4 out of 5 patients. By day 7 the fifth patient showed clinical signs and symptoms of oral mucositis.

For the semiquantification of clinical changes, a cumulative scoring system on a scale of 0 to 5 based on the OMAS scale was used<sup>2,3</sup> (Tables 1 and 2). Figure 2 shows mean OMAS score [standard error (SE)] over time for the five patients included in this preliminary study.

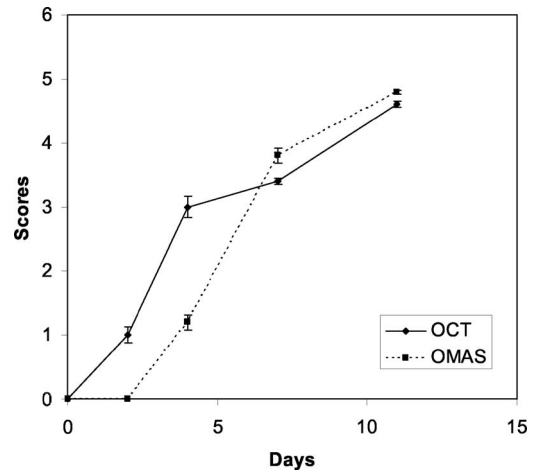


**Fig. 1** *In vivo* OCT images of ventral surface of tongue before (a), after 2 days (b), after 7 days (c), and after 11 days (d) of chemotherapy. In (a), smooth stratified squamous epithelium (1) is visible, separated from the submucosa (2) by the basement membrane (3). Cumulative diagnostic imaging score is 0. In (b), epithelium is thinner by 50%, surface is still intact, although directly below the surface some breakdown is apparent (5). Subepithelial tissues just below the basement membrane show some disruption. At this point, the patient was totally asymptomatic. Cumulative diagnostic imaging score is 2. Further epithelial atrophy is seen after 7 and 11 days [(C) and (D)], with infiltrate around the basement membrane and disruption of the adjacent epithelial and subepithelial tissues (4), and breakdown of the epithelial surface (5). Cumulative diagnostic imaging score for (c) is 3 and for (d) is 5.

**3.2 Imaging Data (Figs. 1 and 2)**

By day 2, 4 out of 5 patients showed signs of mucositis using the OCT-based imaging scale—these were the same patients who developed the first signs of clinical mucositis between days 2 and 4. By day 4, all five patients showed mucositis based on the imaging data. Using imaging, the following events were detected: (1) change in epithelial thickness and loss of subepithelial integrity (day 2 onward), (2) loss of surface keratinized layer continuity (day 4 onward), (3) loss of epithelial integrity (day 7 onward).

Figure 1 shows OCT scans acquired from a patient receiving 5-fluorouracil continuous intravenous (IV) infusion for 4 consecutive weeks. The patient developed clinical grade I mucositis after 4 days and grade II after 8 days. The OCT image acquired 2 days after chemotherapy [Fig. 1(b)] demonstrates mucositis change. Observations include epithelial thinning by

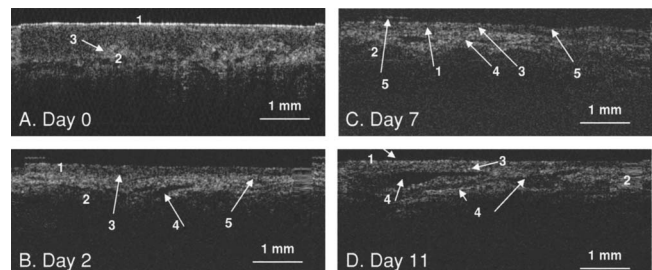


**Fig. 2** OMAS and OCT scores (SE) over time. Day 0 marks the beginning of chemotherapy.

an average of approximately 50% and disruption of the sub-epithelial layers just below the basement membrane. Further epithelial atrophy is seen 7 and 11 days after chemotherapy [Figs. 1(c) and 2(d)], with infiltrate in the area of the basement membrane, disruption of the adjacent epithelial and sub-epithelial tissues, and breakdown of the epithelial surface. The somewhat reduced imaging capability of OCT at days 7 and 11 in the deeper tissues [Figs. 1(c) and 1(d)] may be due to hyperemia in the tissues. Light at 1300 nm is strongly absorbed by blood, mainly due to its water content. Thus mucositis change was detected earlier using OCT imaging than by conventional clinical examination and predicted changes noted later in the visual clinical examination. Imaging artifacts with the appearance of “smearing” are visible on the right side of Fig. 1(a), and the left side of Fig. 1(d).

### 3.3 Comparison of Imaging Scores versus Clinical Mucositis Scores (OMAS)

The imaging data tended to give higher scores compared to clinical scores early on (days 0 to 4—see Fig. 2). However, correspondence was good at days 7 and 11. These data indicate that the imaging-based diagnostic approach was more sensitive to early change than the conventional clinical approach. Once mucositis was established and the clinical manifestation of the condition was more advanced, the imaging and clinical scores converged. Clinically, this finding was highly relevant, as earlier detection of mucositis change will allow the earlier and more effective initiation of antimucositis measures.

## 4 Discussion

Using OCT, noninvasive, rapid, real-time imaging of oral mucosa and identification of structural changes during the development of oral mucositis was possible. The semiquantitative imaging-based scoring system performed well, with the imaging data providing evidence of mucositis prior to clinical findings and showing higher scores early in the course of mucosal damage compared to clinical scores. These findings are important as they suggest that the imaging-based diagnostic method described here is more sensitive to early mucositis than the clinical scoring system and predicts future clinical mucositis. Clinically, this finding is highly relevant, as earlier detection of mucosal damage will allow the potential for earlier intervention and offers the potential for prevention or reduction of severity of mucositis. In addition, OCT imaging may provide more effective investigation of preventive and therapeutic interventions for mucositis. Once mucositis was established and the clinical manifestation of the condition was more advanced, the imaging and clinical scores converged. Two animal studies investigating the use of OCT for detecting and quantifying oral mucositis also reported the potential of using this approach to detect mucositis changes in murine mucosa (1) several days before their clinical manifestation and (2) in cases where the mucositis damage remained subclinical.<sup>30,31</sup>

Although OCT technology is currently limited in its availability to clinicians, its accessibility is increasing rapidly as costs diminish and turnkey systems become available.

## 5 Conclusion

These preliminary studies demonstrate the potential of noninvasive OCT for detecting and semiquantifying oral cancer therapy-induced mucositis. More extensive studies are in progress that will permit a more comprehensive evaluation and statistical analysis of this approach.

### Acknowledgments

This work was supported by Tobacco-Related Disease Research Program Grant No. 14IT-0097 (PWS, MJHW); National Institutes of Health Laser Microbeam and Medical Program Grant No. P41-RR01192 (PWS, MJHW, ZC); and National Institutes of Health Grants No. EB-00255, CA-91717, and RR-01192 (ZC).

### References

1. B. J. Modi, B. Knab, L. E. Feldman, A. J. Mundt, M. Yao, K. B. Pytynia, and J. Epstein, “Review of current treatment practices for carcinoma of the head and neck,” *Expert Opin. Pharmacother.* **6**, 1143–1155 (2005).
2. S. T. Sonis, L. S. Elting, D. Keefe, D. E. Peterson, M. Schubert, M. Hauer-Jensen, and E. B. Rubenstein, “Perspectives on cancer therapy-induced mucosal injury: Pathogenesis, measurement, epidemiology, and consequences for patients,” *Cancer* **100**, 1995–2025 (2004).
3. S. T. Sonis, G. Oster, H. Fuchs, L. Bellm, B. Z. Williamson, J. Edelsberg, D. E. Peterson, M. M. Schubert, F. K. Spijkervet, and M. Horowitz, “Oral mucositis and the clinical and economic outcomes of hematopoietic stem-cell transplantation,” *J. Clin. Oncol.* **19**, 2201–2205 (2001).
4. L. S. Elting and Y. C. Shih, “The economic burden of supportive care of cancer patients,” *Support Care Cancer* **12**, 219–226 (2004).
5. L. S. Elting, C. Cooksley, M. Caambers, S. B. N. Cantor, F. Manzuillo, and E. B. Rubenstein, “The burdens of cancer therapy. Clinical and economic outcomes of chemotherapy-induced mucositis,” *Cancer* **100**, 1324–1326 (2004).
6. J. B. Epstein, P. Stevenson-Moore, S. M. Jackson, J. H. Mohamed, and J. J. Spinelli, “Prevention of oral mucositis in radiation therapy: A controlled study with benzydamine hydrochloride rinse,” *Int. J. Radiat. Oncol., Biol., Phys.* **16**, 1571–1575 (1989).
7. J. B. Epstein, “Infection prevention in bone marrow transplantation and radiation patients,” *NCI Monogr.* **9**, 73–85 (1990).
8. J. B. Epstein, M. M. Schubert, and C. Scully, “Evaluation and treatment of pain in patients with orofacial cancer: A review,” *The Pain Clinic* **4**, 3–20 (1991).
9. J. B. Epstein, “Oral complications of cancer chemotherapy: Etiology, recognition and management,” *Can. J. Oncol.* **2**, 83–95 (1992).
10. K. Bizheva, A. Unterhuber, B. Hermann, B. Povazay, H. Sattman, and A. F. Fercher, “Imaging *ex vivo* healthy and pathological human brain tissue with ultra-high-resolution optical coherence tomography,” *J. Biomed. Opt.* **10**, 011006 (2005).
11. M. E. Brezinski and J. G. Fujimoto, “Optical coherence tomography: High-resolution imaging in nontransparent tissue,” *IEEE J. Sel. Top. Quantum Electron.* **5**, 1185–1192 (1999).
12. P. J. Tadrous, “Methods for imaging the structure and function of living tissues and cells: I. Optical coherence tomography,” *J. Pathol.* **191**, 115–119 (2000).
13. J. A. Izatt, M. D. Kulkarni, K. Kobayashi, M. V. Sivak, J. K. Barton, and A. J. Welch, “Optical coherence tomography for biodiagnostics,” *Opt. Photonics News* **8**, 41–47 (1997).
14. Z. Ding, “High-resolution optical coherence tomography over a large depth range with an axicon lens,” *Opt. Lett.* **27**, 4 (2002).
15. D. Huang, E. A. Swanson, C. P. Lin, J. S. Schuman, W. G. Stinson, W. Chang, M. R. Hee, T. Flotte, K. Gregory, and C. A. Puliafito, “Optical coherence tomography,” *Science* **254**, 1178–1181 (1991).
16. E. A. Swanson, J. A. Izatt, M. R. Hee, D. Huang, C. P. Lin, J. S. Schuman, C. A. Puliafito, and J. G. Fujimoto, “*In vivo* retinal imaging by optical coherence tomography,” *Opt. Lett.* **18**, 1864–1866 (1993).
17. J. G. Fujimoto, M. R. Hee, J. A. Izatt, S. A. Boppart, E. A. Swanson, C. P. Lin, J. S. Schuman, and C. A. Puliafito, “Biomedical imaging using optical coherent tomography,” *Proc. SPIE* **3749**, 402 (1999).

18. B. Bouma, G. J. Tearney, S. A. Boppart, M. R. Hee, M. E. Brezinski, and J. G. Fujimoto, "High-resolution optical coherence tomographic imaging using a mode-locked Ti:Al/sub 2/O/sub 3/ laser source," *Opt. Lett.* **20**, 1486–1488 (1995).
19. P. Wilder-Smith, W. G. Jung, M. Brenner, K. Osann, H. Beydoun, D. Messadi, and Z. Chen, "In vivo optical coherence tomography for the diagnosis of oral malignancy," *Lasers Surg. Med.* **35**, 269–275 (2004).
20. E. Matheny, N. M. Hanna, W. G. Jung, Z. Chen, and P. Wilder-Smith, "Optical coherence tomography of malignancy in the hamster cheek pouch," *J. Biomed. Opt.* **9**, 978–981 (2004).
21. E. Matheny, N. Hanna, R. Mina-Araghi, W. G. Jung, Z. Chen, and P. Wilder-Smith, "Optical coherence tomography of malignant hamster cheek pouches," *J. Investig. Med.* **51**, S78 (2003).
22. S. A. Boppart, M. R. Hee, J. G. Fujimoto, R. Birngruber, C. A. Toth, E. A. Swanson, C. P. Cain, G. D. Noojin, C. D. DiCarlo, and W. P. Roach, "Dynamic evolution and *in vivo* tomographic imaging of laser-induced retinal lesions by using optical coherence tomography," *Presented at IEEE/Proc. CLEO*, May 1995, Baltimore, Md.
23. T. E. Milner, D. Dave, Z. Chen, D. M. Goodman, and J. S. Nelson, "Optical coherence tomography as a biomedical monitor in human skin," in *Optical Society of America (OSA)*, R. R. Alfano and J. G. Fujimoto, Eds., pp. 220–223, OSA, Washington, DC (1996).
24. K. J. Bamford, S. W. James, H. Barr, and R. P. Tatam, "Optical low coherence tomography of bronchial tissue," Chapter 30 in *Advanced Materials and Optical Systems for Chemical and Biological Detection*, M. Fallahi and B. I. Swanson, Eds., pp. 172–179, SPIE, Bellingham, Wash. (1999).
25. P. Wilder-Smith, W. G. Jung, M. Brenner, K. Osann, H. Beydoun, D. Messadi, and Z. Chen, "In vivo optical coherence tomography for the diagnosis of oral malignancy," *Lasers Surg. Med.* **35**, 269–275 (2004).
26. P. Wilder-Smith, K. Osann, N. Hanna, N. E. Abbadi, M. Brenner, D. Messadi, and T. Krasieva, "In vivo multiphoton fluorescence imaging: A novel approach to oral malignancy," *Lasers Surg. Med.* **35**, 96–103 (2004).
27. P. Wilder-Smith, T. Krasieva, W. G. Jung, J. Zhang, Z. Chen, K. Osann, and B. Tromberg, "Non-invasive imaging of oral premalignancy and malignancy," *J. Biomed. Opt.* **10**, 051601 (2005).
28. W. G. Jung, J. Zhang, L. Wang, P. Wilder-Smith, Z. Chen, D. T. McCormick, and N. C. Tien, "Three-dimensional optical coherence tomography employing a 2-Axis MEMS," *J. Biophotonics STQE* **11**, 806 (2006).
29. W. G. Jung, J. Zhang, J. R. Chung, P. Wilder-Smith, M. Brenner, J. S. Nelson, and Z. Chen, "Advances in oral cancer detection using optical coherence tomography," *J. Biophotonics STQE* **11**, 811 (2005).
30. T. M. Muanza, A. Cotrim, M. McAuliffe, A. Sowers, B. Baum, J. Cook, F. Feldchtein, P. Amazeen, C. N. Coleman, and J. B. Mitchel, "Evaluation of radiation-induced oral mucositis by optical coherence tomography," *Clin. Cancer Res.* **11**, 5121–5127 (2005).
31. P. Wilder-Smith, M. J. Hammer-Wilson, J. Zhang, Q. Wang, K. Osann, Z. Chen, H. Wigdor, J. Schwartz, and J. Epstein, "In vivo imaging of oral mucositis in an animal model using optical coherence tomography (OCT) and optical doppler tomography (ODT)," *J. Clin. Cancer Res.* (to be published).